

Modelling a Multi-Faction Conflict in Multi-Domain Operations

Bao Nguyen

Defence R&D Canada and University of Ottawa
101 Colonel By Dr, Ottawa, ON
CANADA
p.bao.u.nguyen@gmail.com

Andrew Gill

Defence Science and Technology Group
PO Box 1500, Edinburgh, SA
AUSTRALIA
andrew.gill@defence.gov.au

Alessio Vaghi

armasuisse Science and Technology
CH-3602, Thun
SWITZERLAND
alessio.vaghi@armasuisse.ch

Vadym Slyusar

Central Research Institute of Armaments and Military Equipment of Armed Forces of Ukraine
Povytrphlotsky Av. 28 B, Kyiv, 03049
UKRAINE
swadim@ukr.net

Bernt Åkesson

Finnish Defence Research Agency
PO Box 10, FI-11311 Riihimäki
FINLAND
bernt.akesson@mil.fi

Esa Lappi

National Defence University, Finland
Department of Military Technology
PO Box 7 FI-00861 HELSINKI
FINLAND
esa.lappi@mil.fi

Stephan Seichter

Bundeswehr Office for Defence Planning
D-82024 Taufkirchen
GERMANY
stephanseichter@bundeswehr.org

Chris Rolfs

Cervus Defence and Security Ltd.
Porto Science Park, Bybrook Road, Porton Down, SP4 0BF Salisbury
UNITED KINGDOM
Chris.r@cervus.ai

Peter Hillmann

Universität der Bundeswehr München
85577 Neubiberg,
GERMANY
peter.hillmann@unibw.de

ABSTRACT

Combat models based on Lanchester equations describe a homogeneous blue force against a red force. However, in reality, a conflict involves multiple factions operating in multiple domains. For example, in the Vietnam War, US force fought alongside the South Vietnamese against the North Vietnamese. With this viewpoint, we provide a general model of attrition of two sides (Blue and Red) each possibly having allies (green etc.). Also nowadays, a conflict does not only occur in the physical domain but also in domains created by new and emerging technologies. For example, cyber strategies are included reflecting today's complexity of multi-domain operations. Our model is probabilistic in the sense that attrition rates obey density distributions and is based on epidemic models. It yields metrics such as the duration of the conflict and the number of casualties. Hence, we compare two scenarios: a) a Blue force against a Red force and b) Blue and Green forces against a Red force. Through Data Farming (MSG-186) analysis of the parameter space, we determine the chance of success of each side and what it takes to win the conflict. This gives us insights into modern warfare involving multi-factions and perhaps estimates the possible outcomes in multi-domain operations.

1.0 INTRODUCTION

Military simulations are useful tools to make predictions about the outcome of conflicts, plan future courses of action, and thus support military decision making. Ensuring these descriptions capture the essential elements of the military operation, the underlying models are becoming increasingly complex. Particularly in multi-faction conflicts, the number of configurable parameters increase significantly, creating a multi-dimensional problem space.

Data Farming is a methodology which combines the rapid prototyping of simulation models with the exploratory power of high-performance computing to quickly generate insight into the problem space. By performing multiple simulation runs, a variety of alternatives can be explored to improve decision makers' situational awareness and provide evidence for informed and robust decisions. This process allows for the consideration of uncertainties and the discovery of unexpected outcomes.

Data Farming has been codified through the efforts of MSG-088 [1] and proof-of-concept applications have been provided by MSG-124 [2]. To make data farming tools readily available, and for a broader audience, MSG-155 developed Data Farming Services (DFS), designed as a mesh of microservices [3]. DFS was tested with two use cases, showing its general applicability [4]. The Data Farming process can be condensed into four main steps: create the scenario, define the parameter values or ranges, run the simulations, analyse, and visualize data. Steps in the process can be repeated as required to further expand the evidence generated from the Data Farming process.

Task group MSG-186, entitled Multi-Dimensional Data Farming, was initiated to demonstrate where Modelling and Simulation can support a multi-model, multi-element, multi-operation simulation approach to understand the uncertainty and complexity of future military challenges. In this paper we explore taking the seminal paper of Lanchester [5] to highlight where Data Farming can further exploit the original research. In [5] the warfare of a Blue force against a Red force is modelled in a deterministic way through the following system of linear differential equations:

$$\frac{dB}{dt} = -r \cdot R \quad \frac{dR}{dt} = -b \cdot B \quad (1)$$

where B (resp. R) is the size of a Blue (resp. Red) force while b is the effectiveness of a Blue force against a Red force (and r vice versa). For $b, r > 0$, the victory condition for a Blue force in this simple model is well known, and depends on only one combined parameter:

$$\varphi = \left(\frac{B_0}{R_0}\right)^2 \cdot \frac{b}{r} > 1 \quad (2)$$

where B_0 (resp. R_0) is the initial size of a Blue (resp. Red) force). Eq. (2) illustrates the famous Lanchester ‘square law’, i.e., a doubling of Blue’s initial force size (B_0) would require a four-fold increase in Red’s weapon effectiveness (r) to compensate.

1.1 Probability of Victory

Due to unexpected events, military operations are usually affected by a given degree of uncertainty. That is, the sizes of the forces are reasonably known but the effectiveness as encoded in the attrition coefficients b and r fluctuate as they depend on many factors such as the time, environment, technologies and morale [6]. Hence, we allow b and r to each follow a probability distribution. The victory condition for a Blue force can be rearranged to $Z = r - b' < 0$, where $b' = (B_0/R_0)^2 \cdot b$. If b and r each follow independent gamma distributions with probability density functions $f_b(x; k_b, \theta_b)$ and $f_r(x; k_r, \theta_r)$, then the probability that a Blue force wins can be explicitly calculated [7]:

$$P_B = P(Z < 0) = \frac{\chi^{k_r}}{k_r \cdot (1 + \chi)^{k_r + k_b}} \cdot \frac{{}_2F_1\left(1, k_r + k_b, k_r + 1; \frac{\chi}{1 + \chi}\right)}{B(k_r, k_b)} \quad (3)$$

where ${}_2F_1(a, b, c; z)$ is the ordinary hypergeometric function, $B(z_1, z_2)$ is the beta function and:

$$\chi = \left(\frac{B_0}{R_0}\right)^2 \cdot \frac{\theta_b}{\theta_r} \quad (4)$$

Thus, the probability of the Blue force winning depends on only three independent model parameters, the two gamma distribution shape parameters k_b and k_r and a combined parameter χ . Note that Eq. (4) is a probabilistic generalization of Eq. (2). Figure 1-1 (a) illustrates examples of the gamma density distribution. Figure 1-1 (b) displays P_B as a function of B_0/R_0 and θ_b/θ_r , assuming $k_b = k_r = 9$. The contour lines of equal probability reflect the relationship between these parameters encoded in χ in Eq. (4). The white line corresponds to $\varphi = 1$. In the deterministic case, the area of Figure 1-1 above (resp. below) the white line represents the situation where the Blue force wins (resp. loses).

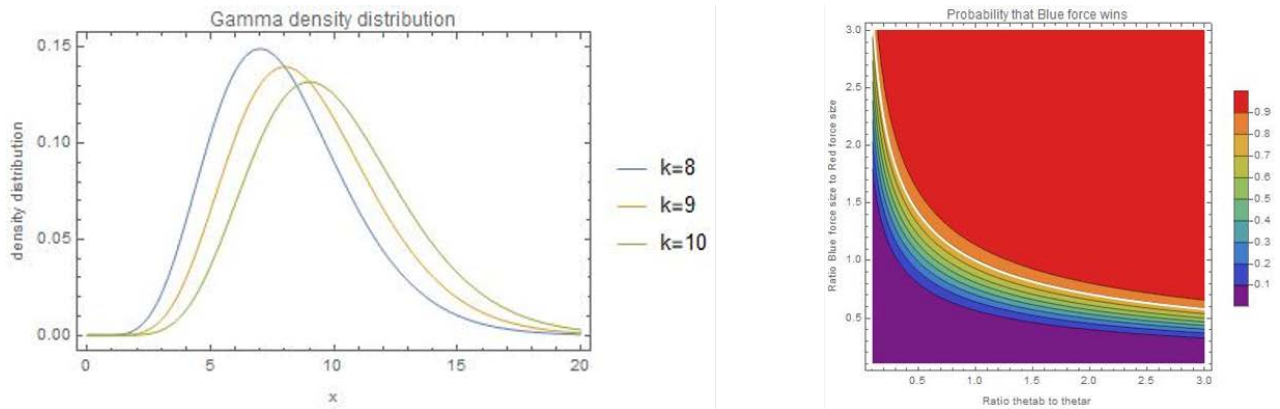


Figure 1-1: (a) Examples of gamma density distribution $f(x; k; \theta)$ for $k = 8, 9, 10$. (b) Contour plot of the probability that Blue force wins P_B as a function of B_0/R_0 and θ_b/θ_r .

There are two ways to increase P_B . The first way is for a Blue force to outnumber a Red force, i.e., large $B_0/R_0 > 1$. The second way is for a Blue force to have better weapons than those of a Red force, namely large $\theta_b/\theta_r > 1$. For example, if $B_0/R_0 = 3$ then $P_B \geq 0.9$ for $\theta_b/\theta_r \geq 0.1$ which confirms the general planning assumption of a force ratio of 3 to 1 (as used in military planning of requiring a force ratio of 3:1 to conduct an offensive rural operation against a hasty defence). That is, if a Blue Force is three times a Red force, then a Blue force wins. Similarly, if $\theta_b/\theta_r = 3$ then $P_B \geq 0.8$ for $B_0/R_0 > 0.7$. If both $B_0/R_0 \geq 1.2$ and $\theta_b/\theta_r \geq 1.2$ then $P_B \geq 0.9$. Note that if $B_0/R_0 = \theta_b/\theta_r = 1$, i.e., the size of the Blue force equals the one of the Red force and the effectiveness of Blue force weapons equals the one of Red force weapons, then as expected $P_B = 1/2$. This result is independent of the density distribution if b and r follow the same density distribution [8].

2.0 MULTI-FACTION MODEL

Historically, warfare often involves more than two factions [9]. For example, in the Vietnam war, South Vietnam fought alongside the United States of America (USA) against North Vietnam. In the Afghan war, there were Afghanistan Allies who fought along the USA against the Taliban. However, Lanchester equations model Blue force against Red force only. To accommodate reality, we extend Lanchester model to include a Green force:

$$\frac{dB}{dt} = -r_b \cdot R \quad \frac{dR}{dt} = -b \cdot B - g \cdot G \quad \frac{dG}{dt} = -r_g \cdot R + \alpha \cdot R \quad (5)$$

In this paper, a Green force is an ally of a Blue force. The term $\alpha \cdot R$ incorporates the rate at which the allies supply weapons to a Green force in a way that is proportional to the current Red force. With the help of a Green force, a Blue force has a better chance to win against a Red force. In this model one can reformulate a Green force in terms of a Blue force. Defining $r'_g = r_g - \alpha$ (note that r'_g may be negative) one gets

$$\frac{dB}{dt} = -r_b \cdot R \quad \frac{dR}{dt} = -\frac{\lambda^2}{r_b} \cdot B + \frac{g \cdot \Delta}{r_b} \quad G(t) = G_0 + \frac{r'_g}{r_b} (B(t) - B_0) \quad (6)$$

where $\lambda^2 = b \cdot r_b + g \cdot r'_g$ and $\Delta = r'_g \cdot B_0 - r_b \cdot G_0$, and either may be positive or negative. Note that once B is known also G is known: the influence of a Green force is now captured through g, λ and Δ .

2.1 Analytical Solutions

The force trajectory curves are the solutions to Eq. (6). For $\lambda^2 > 0$ these are hyperbolic:

$$R(t) = R_0(\cosh(\lambda t) - \phi \cdot \sinh(\lambda t)) \quad (7)$$

$$B(t) = \frac{g \cdot \Delta}{\lambda^2} - \frac{r_b R_0}{\lambda} (\sinh(\lambda t) - \phi \cdot \cosh(\lambda t)) \quad (8)$$

where $\phi = \frac{b \cdot B_0 + g \cdot G_0}{R_0 \cdot \lambda} > 0$. For $\lambda^2 < 0$ they are trigonometric:

$$R(t) = R_0 (\cos(\bar{\lambda} t) - \bar{\phi} \cdot \sin(\bar{\lambda} t)) \quad (9)$$

$$B(t) = -\frac{g \cdot \Delta}{\bar{\lambda}^2} - \frac{r_b R_0}{\bar{\lambda}} (\sin(\bar{\lambda} t) + \bar{\phi} \cdot \cos(\bar{\lambda} t)) \quad (10)$$

with $\bar{\phi} = \frac{b \cdot B_0 + g \cdot G_0}{R_0 \cdot \bar{\lambda}} > 0$ and $\bar{\lambda} = |\lambda|$. For $\lambda^2 = 0$ they are polynomial:

$$R(t) = R_0 + \frac{g \Delta}{r_b} t \quad (11)$$

$$B(t) = B_0 - r_b R_0 t - \frac{g \Delta}{2} t^2 \quad (12)$$

For illustrations, we plot the sizes of a Blue force, a Red force and a Green force as a function of time with λ^2 positive in Figure 2-1. Blue wins in the scenario of Figure 2-1.

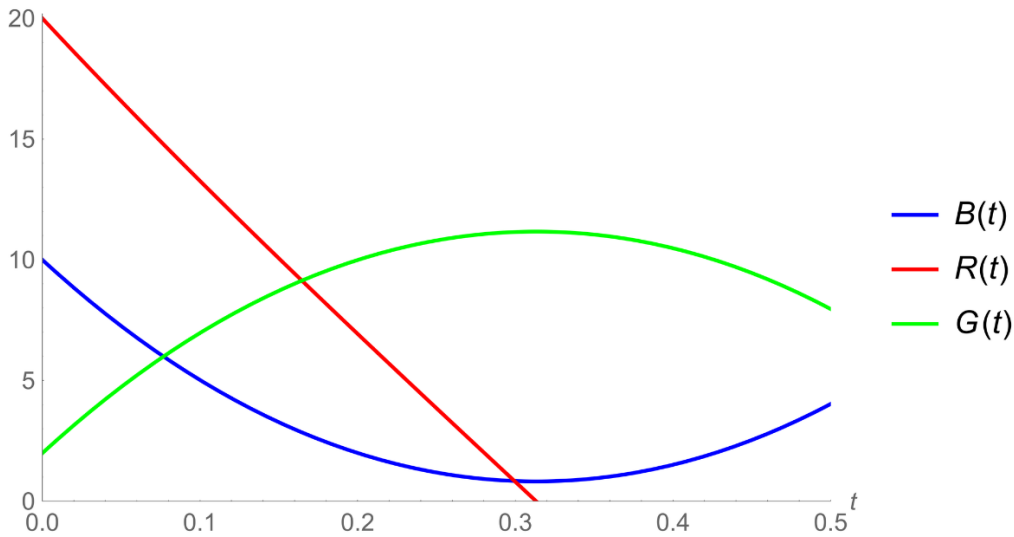


Figure 2-1: Blue, Red and Green force size as functions of time for $\lambda^2 > 0$. We have chosen the parameters so that the Blue force wins even though the Red force outnumbers the Blue force by a factor of 2: $R_0 = 20$, $B_0 = 10$ and $G_0 = 2$. We set $b = 6$, $r_b = 3$, $r_g = 3$, $\alpha = 6$ and $g = 5$ so that $r'_g = -3$, $\lambda^2 = 6$, $\phi = 7/(2\sqrt{3})$ and $\Delta = -36$.

2.2 Victory Condition

The advantage of reformulating $G(t)$ in terms of $B(t)$ is that the system of Eq. (6) consists of just two linear differential equations which are separable. Depending on the value of λ , these equations can be rewritten in a form representing a conic section. If $\lambda^2 > 0$ (resp. $\lambda^2 < 0$) they represent a hyperbola (resp. an ellipse):

$$\left(B(t) - \frac{g \cdot \Delta}{\lambda^2}\right)^2 - \frac{r_b^2}{\lambda^2} R^2(t) = \left(B_0 - \frac{g \cdot \Delta}{\lambda^2}\right)^2 - \frac{r_b^2}{\lambda^2} R_0^2 \quad (13)$$

If $\lambda^2 = 0$, they represent a parabola

$$R^2(t) = -\frac{2 \cdot g \cdot \Delta}{r_b^2} B(t) + \frac{2 \cdot g \cdot \Delta}{r_b^2} B_0 + R_0^2 \quad (14)$$

From these phase space equations, one can determine a victory condition for a Blue force. By requiring $R(t^*) = 0$ and $B(t^*) > 0$ for some finite time t^* , one obtains:

$$\frac{\lambda^2 \cdot B_0^2 - r_b^2 \cdot R_0^2}{2 \cdot g \cdot B_0} > \Delta \quad (15)$$

Hence, if the above inequality holds, a Blue force wins. To show this explicitly, one can reformulate Eq. (15) in terms of the original model parameters:

$$\varphi > 1 + \left(\frac{B_0}{R_0}\right)^2 \cdot \frac{g}{r_b} \cdot \left(\frac{r'_g}{r_b} - 2 \cdot \frac{G_0}{R_0}\right) \quad (16)$$

Now, it is apparent how the victory condition of the original Lanchester model (i.e., $\varphi > 1$) is modified by the introduction of a Green force. In particular, the sign of the last bracketed term mostly determines whether a Blue force wins or not. If the initial support from Green is sufficiently large (i.e., $G_0/B_0 > r'_g/2r_b$) then a Blue force is facilitated to win (N.B. if $r'_g < 0$, this is always the case). Depending on the magnitude of g (the effectiveness of a Green force against Red), a Blue force is even more facilitated to win.

Alternatively, one can express the victory condition Eq. (15) as a function relating B_0/R_0 and b/r_b :

$$\frac{B_0}{R_0} > \left(\sqrt{\frac{b}{r_b} - \frac{g}{r_b} \cdot \frac{r'_g}{r_b} + \left(\frac{g}{r_b} \cdot \frac{G_0}{R_0}\right)^2} - \frac{g}{r_b} \cdot \frac{G_0}{R_0} \right) / \left(\frac{b}{r_b} - \frac{g}{r_b} \cdot \frac{r'_g}{r_b} \right) \quad (17)$$

In this way, we can better study the implication of the initial support from Green. In Figure 2-2 we plot B_0/R_0 as a function of b/r_b according to the victory condition Eq. (17). Figure 2-2(a) (resp. Figure 2-2(b)) represents the victory condition for $g/r_b = 1$ (resp. $g/r_b = 0.5$). Note that, if either the initial support from Green G_0 or the weapon effectiveness of Green against Red g/r_b is insufficient, there is a critical threshold of Blue's weapon effectiveness against Red (b/r_b) below which Blue can never win, irrespective of any initial force ratio advantage. This phenomenon only occurs in the multi-faction model.

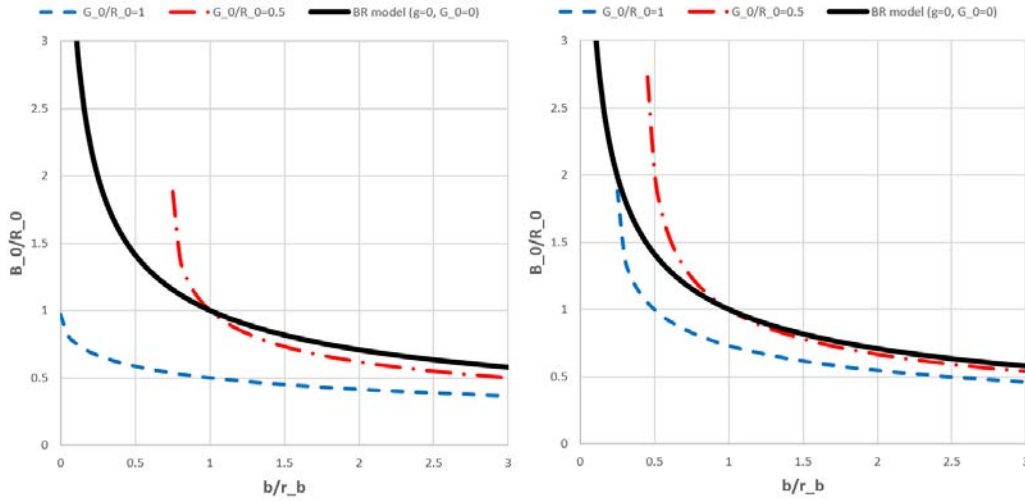


Figure 2-2: Victory condition for Blue in the multi-faction model in terms of B_0/R_0 as a function of b/r_b for (a) $g/r_b = 1$ and (b) $g/r_b = 0.5$. Here, $r'_g/r_b = 1$ and we consider two possible values of the initial support from Green given by $G_0/R_0 = 1$ (dashed blue lines) and $G_0/R_0 = 0.5$ (dot-dashed red lines). Black lines represent the victory condition according to the original Lanchester model given by Eq. (2).

2.3 Probability of Victory

The victory condition Eq. (15) can also be rearranged to:

$$Z = \frac{b}{r_b} - \frac{g}{r_b} \cdot \left(\frac{r_g}{r_b} - \frac{\alpha}{r_b} \right) + 2 \cdot \frac{G_0}{B_0} \cdot \frac{g}{r_b} - \frac{R_0^2}{B_0^2} > 0 \quad (18)$$

so that the probability that a Blue force wins is defined as:

$$P_B = P(Z > 0) = \int_0^\infty f_{g/r_b}(g') \int_0^\infty f_{r_g/r_b}(r') \int_0^\infty f_{\alpha/r_b}(\alpha') \int_0^\infty f_{b/r_b}(b') \cdot H \left(b' - g' \cdot (r' - \alpha') + 2 \cdot \frac{G_0}{B_0} \cdot g' - \frac{R_0^2}{B_0^2} \right) \cdot db' \cdot d\alpha' \cdot dr' \cdot dg' \quad (19)$$

where each $f_x(z)$ is an appropriate probability density function for the ratio of the two random parameters, and where $H(x)$ is the Heaviside step function (one if $x > 0$ and zero otherwise). If, as before, we assume each random variable follows independent gamma distributions, the ratio of two independent gamma distributions is known to follow a generalized beta prime distribution with shape parameter equal to one (also called a compound gamma distribution).

While for the Lanchester model, the integrals defining P_B can be analytically calculated in terms of special functions, the introduction of a Green force complicates this calculation significantly. Instead, we can approximate P_B using Monte Carlo sampling according to the gamma density functions for b, r_b, g, r_g and α , and simply record the proportion of times Eq. (18) holds, or use numerical quadrature to approximate the integral in Eq. (19).

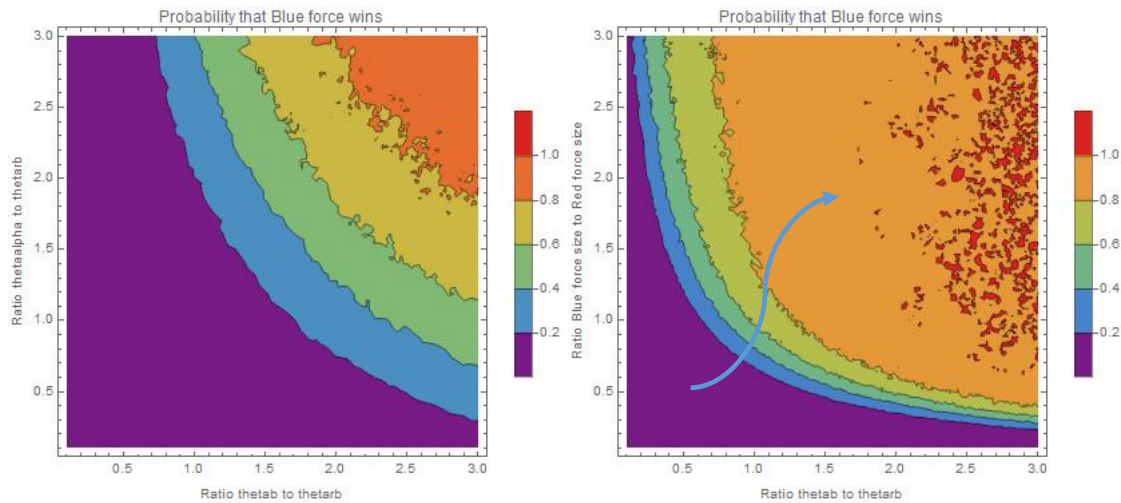


Figure 2-3: Probability that Blue force wins as a function of (a) $\theta_\alpha/\theta_{r_b}$ and θ_b/θ_{r_b} ($= \frac{\theta_g}{\theta_{r_b}}$) with $G_0 = 2$ and (b) $\frac{B_0}{R_0}$ and $\frac{\theta_b}{\theta_{r_b}}$ ($= \frac{\theta_g}{\theta_{r_b}} = \frac{\theta_\alpha}{\theta_{r_b}}$) with $G_0 = 0$.

Regarding Figure 2-3(a), since the mean of a gamma density distribution is $k \cdot \theta$, we could think of the mean having similar effects as the deterministic attrition coefficients e.g., $b \sim k_b \cdot \theta_b$. By assuming the same value of k for all density distributions, the ratio of the attrition coefficients is similar to the ratio of the scale parameters θ , e.g., $\alpha/r_b \sim \theta_\alpha/\theta_{r_b}$. Therefore, as $\theta_\alpha/\theta_{r_b}$ and $\theta_b/\theta_{r_b} = \theta_g/\theta_{r_b}$ a Blue force increases the probability of winning. This means that even though a Blue force is initially outnumbered by a Red force by a factor of two, it is still possible for a Blue force to win if it has sufficient support from a Green force.

This support is not only in the size of the Green force but is also reflected in the multidimensional warfare. That is, if a Blue force and a Green force have superior technologies then both $\theta_\alpha/\theta_{r_b}$ and $\theta_b/\theta_{r_b} = \theta_g/\theta_{r_b}$ increase which increases the probability that a Blue force wins. This could be attributed to better weapons or better communications for example. Also, if a Blue force and/or a Green force can conduct a cyber-attack against a Red force, weakening their weapon effectiveness, the same effect will occur.

Figure 2-3(b) displays the probability that Blue force wins assuming $G_0 = 0$, and is like Figure 1-1. However, a Green force is also fighting against a Red force according to Eq. (5) and therefore P_B is larger than in Figure 1-1. In Figure 2-3(b), a Blue curve depicts a possible path that will improve P_B . Mathematically, the curve of steepest descent/ascent is along the gradient of P_B as a function of its variables. In reality, such a blue path is associated with multiple costs, e.g., the support from a Green force. That path also depends on available technologies, their effectiveness and how the technologies function together. For example, a cyber-attack by a Blue-Green force could reduce the effectiveness of a Red force. Also, if a Green force has access to modern weapons, then the effectiveness of a Green force could increase.

Improvements in size are reflected in B_0, G_0, R_0 while improvements in effectiveness are reflected in the probability density function hyper-parameters of the attrition coefficients b, g, r_g and r_b . In a multi-faction conflict, with sufficient support from an ally (a Green force), a Blue force could overcome a powerful Red force. This support is modelled through the parameter α , and the characteristics of such a pathway will rely on multi-dimensional Data Farming.

3.0 MULTI-DOMAIN MODEL

The multi-faction model Eq. (5) operates solely in the physical domain. To accommodate the cyber domain, we consider the Blue force composed by army systems interconnected by a peer-to-peer network susceptible to cyber attacks. These cyber attacks (hereafter, simply called virus) spread among the army systems like an infection reducing the effectiveness of the infected units. As a countermeasure, the Blue force may employ cyber defence tactics which immunize susceptible and infected units against the virus. To describe the possible spread of the virus [10, 11] we extend the classical epidemic models [12, 13]. Following [14] we decompose the Blue force into compartments

$$B(t) = B_1(t) + B_2(t) + B_3(t) \quad (20)$$

where $B_j = B_j(t)$, $j = 1, \dots, 3$ correspond to the number of susceptible, infected and recovered units, respectively. Then, in the cyber domain we assume three possible transitions between compartments:

$$\begin{aligned} B_1 &\rightarrow B_2 \text{ a susceptible Blue unit is infected by the virus} \\ B_1 &\rightarrow B_3 \text{ a susceptible Blue unit is raised to be immune against the virus} \\ B_2 &\rightarrow B_3 \text{ an infected Blue unit is recovered and raised to immune against the virus} \end{aligned} \quad (21)$$

Incorporating this cyber domain into Eq. (5) yields:

$$\frac{dB_1}{dt} = \left[-\beta_V \cdot B_2 - \beta_A \cdot B_3 - r_b \cdot \frac{R}{B} \right] B_1 \quad (22)$$

$$\frac{dB_2}{dt} = \left[+\beta_V \cdot B_1 - \beta_A \cdot B_3 - r_b \cdot \frac{R}{B} \right] B_2 \quad (23)$$

$$\frac{dB_3}{dt} = \left[+\beta_A(B_1 + B_2) - r_b \cdot \frac{R}{B} \right] B_3 \quad (24)$$

$$\frac{dR}{dt} = -b_{r,A}(B_1 + B_3) - b_{r,V} \cdot B_2 - g_r \cdot G \quad (25)$$

$$\frac{dG}{dt} = -r'_g \cdot R \quad (26)$$

Here, the non-negative parameter β_V (resp. β_A) originates from the part of the model describing the cyber domain and it is related to the occurrence rate of the virus infection (resp. the immunization) within the Blue force. The non-negative parameter $b_{r,V}$ (resp. $b_{r,A}$) encodes the weapon effectiveness of the infected (resp. susceptible and recovered) Blue units against the Red force in the physical domain. In general, $b_{r,V} \leq b_{r,A}$ since the infected units are less effective against the Red force. Note that in this version of the model the Red force is unaffected by the virus.

Figure 3-1 displays the solution of Eq. (22-26) where we have chosen values of the parameters to allow comparison with the results in Figure 2-1. Note that in general, the virus infection by the Red force reduces the Blue force and delays the Blue victory. Conversely, the Green force, being unaffected by the cyber attack, reaches a larger number of units compared with Figure 2-1.

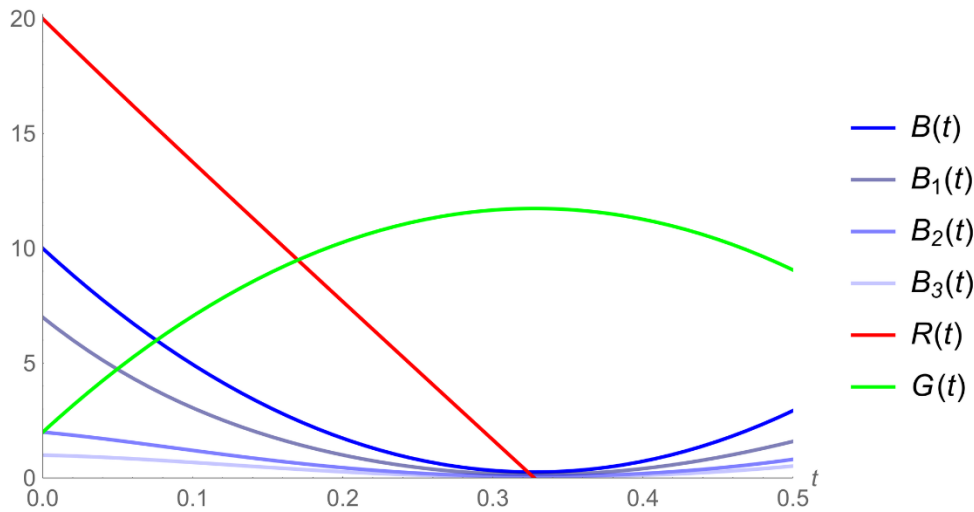


Figure 3-1: Blue, Red and Green force size as functions of time as solutions of Eq. (22-26). Here $B_1(0) = 7$, $B_2(0) = 2$, $B_3(0) = 1$, so that $B(0) = 10$, while $R(0) = 20$ and $G(0) = 2$. The values of the attrition parameters are: $r_b = 3$, $b_{r,A} = 6$, $b_{r,V} = 3$, $g_r = 5$, $r'_g = -3$. The parameters describing the virus infection and immunization value: $\beta_V = 0.5$ and $\beta_A = 0.5$.

4.0 DATA FARMING

While the simple Lanchester model Eq. (1) is completely solvable and the probability of Blue force winning is analytically tractable Eq. (3), extensions to accommodate the multi-faction (Eq. (5)), probabilistic (Eq. (19)), and multi-domain (Eq. (22-26)) aspects of contemporary military operations underpin the requirement for efficient Data Farming analyses as described in the introduction.

For example, if the eight parameters of the multi-faction, multi-domain model Eq. (22-26) each follow a distribution characterised by two hyper-parameters (e.g., the scale and shape parameters of the gamma distribution), then together with the five initial force sizes of Blue, Red and Green, this represents a twenty-one dimensional factor space that influences whether a Blue force wins or not.

If we wanted to fit a fully second-order logistic regression meta-model (to identify non-linearity and combat multipliers) this would require determining 21 main effects, 21 quadratic terms, and 210 two-factor interactions (252 meta-model coefficients in total). This will require an efficient design of experiment of the parameter space, effective analysis tools, and explainable visualizations to provide military decision makers with timely, relevant, and robust data-driven insights.

5.0 SUMMARY

This paper has illustrated the influence that allies (Green force) may have on the outcome of a conflict between a Blue force and a Red force, in that, based on the magnitude and the timeline of the support from the allies, an initially weaker Blue force could overcome an initially stronger Red force. Although our approach is still theoretical and lacks details, it provides a pathway to analyse multi-faction conflicts.

By including additional fidelity, e.g., land force, maritime force, and air force, we could in principle determine the level of support required from a Green force such that a Blue force could win against a Red force. The approach could also be generalized to the case of coalition confrontations, where many additional participants are considered as third parties to the conflict, taking situationally different influences on the intensity and direction of the dynamics of hostilities.

However, as the complexity of models increases, so do their input parameters. For the calculation of results and predictions, Data Farming provides the necessary toolbox so that appropriate conclusions can be drawn. Through multi-dimensional Data Farming, we hope to discover new possibilities that may not be obvious but may be present in modern technologies and their combinations and give us further insights of multi-domain operations in multi-faction conflicts. Task group MSG-186, through its program of work, is progressing towards that end.

Clearly, substantial work lies ahead of us to understand the dynamics of multi-faction conflict in multi-domain operations. However, we believe it is a worthwhile endeavour as multi-faction conflicts have occurred so many times in the history of humanity.

ACKNOWLEDGEMENTS

We extend our appreciation to Maude Amyot-Bourgeois for her comments on the paper.

REFERENCES

- [1] Task Group MSG-088. Data Farming in Support of NATO – Final Report of Task Group MSG-088. STO Technical Report STO-TR-MSG-088. Neuilly-Sur-Seine, France: NATO Science and Technology Organization, 31st March 2014. ISBN: 978-92-837-0205-4. DOI: 10.14339/STO-TR-MSG-088.
- [2] Task Group MSG-124. Developing Actionable Data Farming Decision Support for NATO – Final Report of MSG-124. STO Technical Report STO-TR-IST- 163. Neuilly-sur-Seine, France: NATO Science and Technology Organization, 30th July 2018. ISBN: 978-92-837-2151-2. DOI: 10.14339/STO-TR-MSG-124.
- [3] Huber D, Horne G, Hodicky J, Kallfass D, De Reus N (2019) Data Farming Services: Micro-Services for Facilitating Data Farming in NATO, in: N. Mustafee, K.-H. G. Bae, S. Lazarova-Molnar, M. Rabe, C. Szabo P, Haas Y-J S (Eds.), Proceedings of the 2019 Winter Simulation Conference.
- [4] Seichter S, Akesson B, Richter M and Muts N (2020) Data Farming Services (DFS) for Analysis and Simulation-based Decision Support, CA2X2 Forum 2020 Papers Collection. Rome, Italy: The NATO Modelling and Simulation Centre of Excellence, 2021, pp. 120–128.
- [5] Lanchester FA (1916) Aircraft in warfare: the dawn of the fourth arm, Constable, London, pp. 39-66.
- [6] Kress M, Lin KY and Mackay NJ (2018) The attrition dynamics of multilateral war, Journal of Operations Research, Volume 66 Issue 4: pp. 950-956.
- [7] Gradshteyn IS, Ryzhik IM (2007). Table of integrals, series, and products. Elsevier/Academic Press, Amsterdam. ISBN: 978-0-12-373637-6; 0-12-373637-4.
- [8] Ross S (2010) A First Course in Probability, Pearson Prentice Hall, p.270.
- [9] Kress M (2020) Lanchester Models for Irregular Warfare, *Mathematica*, 8, 737.
- [10] Nguyen BU (2017) Modelling cyber vulnerabilities using epidemic models, 7th international conference on simulation and modelling methodologies, technologies and applications.

- [11] Slyusar, V (2020). On the Issue of Assessing the Effectiveness of Air Defense Based on a Pandemic Model, EasyChair preprint 4173, September 2020, <https://easychair.org/publications/preprint/kLWP>.
- [12] Kermack WO, McKendrick AG (1927) A Contribution to the Mathematical Theory of Epidemics. *Proceedings of the Royal Society A*. 115 (772): 700–721.
- [13] Harko T, Lobo FSN, and Mak MK (2014) Exact analytical solutions of the Susceptible-Infected-Recovered (SIR) epidemic model and of the SIR model with equal death and birth rates. *Applied Mathematics and Computation* 236: 184–194.
- [14] H. C. Schramm and D. P. Gaver, (2013) *Lanchester for cyber: the mixed epidemic-combat model*, Wiley online library.